

Design and Evaluation Methodology for Insulation Systems of Low Voltage Drives with Preformed Coils

Florian Pauli
Institute of Electrical Machines (IEM)
RWTH Aachen University
Aachen, Germany
florian.pauli@iem.rwth-aachen.de

Michael Schröder
Institute of Electrical Machines (IEM)
RWTH Aachen University
Aachen, Germany

Kay Hameyer
Institute of Electrical Machines (IEM)
RWTH Aachen University
Aachen, Germany

Abstract—The high copper fill factor of electrical machines with preformed coils allows for high torque and power densities. However, due to the manufacturing process, completely new challenges arise for the insulation system of machines with such preformed coils. Due to the complex geometry of the coil, conventional enameling processes, which are used in wire wound machines, are not suitable. Therefore, forming of enameled wire, as well as powder coating of already formed bare copper coils, are studied in this work as alternatives.

Keywords—preformed coils, insulation system

I. INTRODUCTION

In electrical machines operating at low speed, such as wheel hub machines, a high torque density is required. Increasing the continuous torque of an electrical machine can be realized by increasing the maximum permissible continuous current which is defined by the thermal limits of the machine's winding insulation system. One option to increase the maximum allowed current is to decrease the losses of the machine. This can be achieved by a high copper fill factor. Due to the round shape of the usually applied conductors, the theoretical maximum mechanical fill factor of electrical machines with conventional round wires is limited to 0.907 for an orthocyclic winding, while rectangular wires can reach the theoretical mechanical factor of 1. For this consideration however no insulation is regarded. In actual slots of low voltage machines with round wires, the electrical copper fill factor is practically limited to about 60 % [4]. Using the shaped coil which is studied in the scope of this paper, an electrical copper factor of more than 70 % is achieved.

In order to utilize the entire cross section of the slot, conical coils are produced. In [5] a casting process to manufacture such coils from copper or aluminum is introduced. The coils studied here are made of copper and produced in a forming process [1].

The primary insulation of such coils must be studied in particular. Conventional insulation processes for round wires are not applicable for preformed coils. Preformed coils have been applied in high voltage machines for decades [6]. The requirements for an insulation system of a low voltage machine however differ. High voltage machines are either

This research and development project is funded by the German Federal Ministry of Education and Research (BMBF) within the Framework Concept "Serienflexible Technologien für elektrische Antriebe von Fahrzeugen 2". The authors are grateful to the BMBF for the financing of this collaboration and are responsible for the contents of this publication.

Furthermore, we want to thank our project partners Schaeffler AG, Breuckmann GmbH and the Institute of Metal Forming (IBF) from RWTH Aachen University for the excellent collaboration concerning this project.

tailormade or built in small numbers. The degree of automation in the production process is therefore much lower than for low voltage machines. The application of the primary insulation which is considered in this paper must therefore be suitable for automatization. Furthermore, the insulation system of high voltage machines can withstand partial discharge (PD) [12]. The insulation system of low voltage machines is designed to be PD free at any operating point. To ensure that the insulation system for the preformed coil is PD free, qualification tests based on the standards [2, 10] are performed.

II. COIL GEOMETRY

In Fig. 1, the geometry of the coil which is used as a test device for the insulation system is displayed alongside with a conventional round wire winding. To ensure high copper fill factors, the conductors, which are close to the slot ground, are wider than those close to the slot opening.

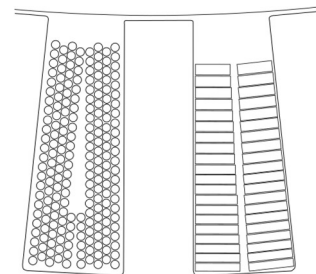


Fig. 1: Slot geometry with conventional round wire (left) and preformed coil (right).

The coil is manufactured from of a bare copper wire by a forming process [1]. During the production process, large force is applied upon the semi-finished coil arrangement (Fig. 2, left) made of rectangular copper wire. The resulting coil is displayed in Fig. 2, right. Due to its shape, the coil is not suitable for a conventional process of enamel application.

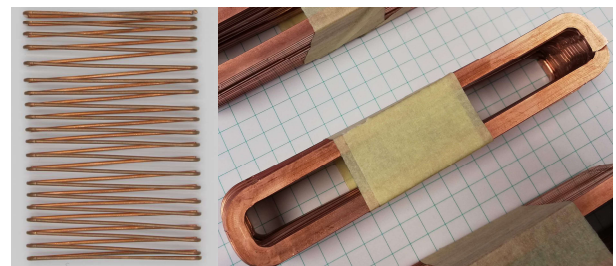


Fig. 2: Semi-finish (left) and preformed coil without primary insulation (right).

III. APPLICATION OF PRIMARY INSULATION

Conventional enameled wires are insulated in a continuous process. The wire is unwound from one coil and passes alternately a station where the enamel is applied and an oven, where it is hardened (Fig. 3). Using this procedure several thin layers of enamel are applied.

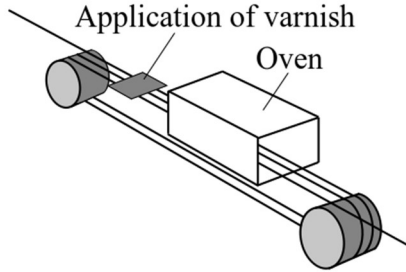


Fig. 3: Visualization of the varnish application for enameled wires.

Due to the geometry of the preformed coil, such a continuous process is not applicable in this study. The minimum insulation thickness of enameled wires depends on the diameter. It is given for different insulation grades and wire diameters in Tab. I.

TABLE I. INSULATION THICKNESS FOR VARIOUS WIRE DIENSIONS

Nominal diameter in mm	Minimum insulation thickness in μm		
	Grade 1	Grade 2	Grade 3
1.0	4.0	8.0	11.5
2.0	7.0	13.5	19.5
4.0	10.5	20.0	30.0

For the test coils studied in this paper an electrical copper fill factor $>70\%$ is aimed. Subsequently the insulation thickness of the test coils must not exceed $80\ \mu\text{m}$. Beside its dimensions and its electrical properties, the insulation system is defined as mentioned before by its thermal class. Conventional enameled wires of modern low voltage machines achieve temperature classes of H up to $180\ ^\circ\text{C}$ or N up to $200\ ^\circ\text{C}$. In the following, two different concepts for the primary insulation of preformed coils are studied:

- Concept A: Standard enameled wire is used in the forming process, resulting in large mechanical stress on the primary insulation.
- Concept B: The insulation material is applied after the forming process.

In both cases, the physical dimensions as well as thermal and electrical properties of the primary insulation are considered. For concept A enameled wires with primary insulations made of polyamide and polyester-imide are considered. For concept B an epoxy coating is studied. In [13] and [14] epoxy powder coatings are studied as a substitute for conventional slot liners. A minimum achievable coating thickness is given of $80\ \mu\text{m}$ is given, which is significantly thinner than conventional slot liners but thicker than the enamel of conventional enameled copper wires.

IV. SPECIMEN PRODUCTION AND INITIAL EVALUATION OF THE PRIMARY INSULATION

A means to evaluate the electrical properties of the primary insulation of low voltage machines is the partial discharge inception voltage (PDIV). When round shaped wires are studied, twisted pair probes are employed for the measurements. For wires with a rectangular cross section, specimens as displayed in Fig. 4 are used.



Fig. 4: Specimen for PDIV measurement of enameled rectangular wires [8].

The bending in the stator end winding is expected to be the weakest point of the primary insulation. Thus, it must be considered when specimens for the PD measurement are designed.

For concept A, L-shaped conductors made of formed flat wires are taped together (Fig. 5, left). For concept B, semi-finished coils are coated, cut in pieces and taped together (Fig. 5, right). Subsequently, the PDIV is measured.

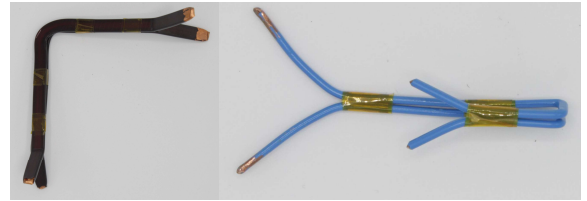


Fig. 5: Specimens for concept A (left) and concept B (right).

The PDIV which is measured for the specimens that are displayed in Fig. 5 is not the same voltage measured for a complete stator winding. While for conductor arrangements the test voltage U_{test} equals the voltage drop across the studied insulation layer U_{cond} , for electrical machines or motorettes, the voltage drop differs (Fig. 6).

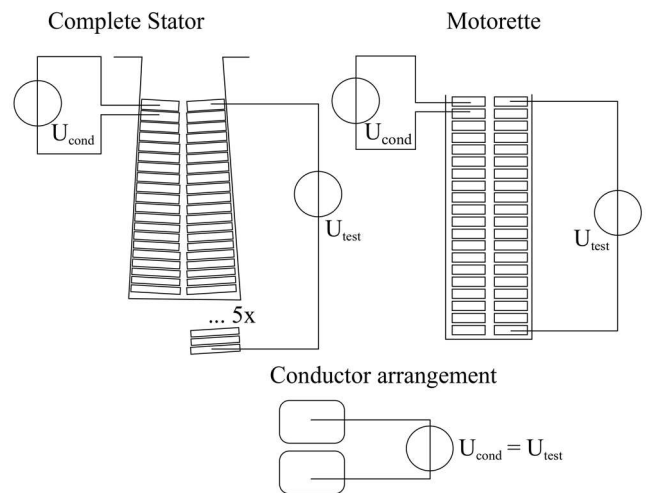


Fig. 6: Voltage drop between two neighboring conductors U_{cond} and applied test voltage U_{test} .

In the standard [2] a methodology is given to calculate the PDIV of an electrical machine from measurements of conductor arrangements. Several empirical based safety factors are used to calculate the PDIV of an inverter driven electrical machine at its maximum operating temperature from measurements of new specimens at room temperature:

$$U_{pkpk,min} = 2 \cdot U_{dc} \cdot a \cdot OF \cdot NF \cdot PD \cdot AF \cdot TF. \quad (1)$$

The calculated PDIV $U_{pkpk,min}$ is a peak-to-peak voltage. It depends on the dc link voltage U_{dc} and the following safety factors:

- a : The voltage drop between two neighboring conductors is only a part of the terminal voltage – $a \leq 1$.
- OF : Particularly at machines that are connected to the inverter using long cables, overshoot occurs at the machine terminals – $1.1 \leq OF \leq 2.5$.
- NF : The battery voltage can deviate from its nominal voltage – $NF = 1.1$.
- PD : The PDIV is greater than the partial discharge extinction voltage (PDEV). To ensure a PD free winding at all times, the operating voltage should not exceed the PDEV – $PD = 1.25$.
- AF : Consideration of ageing – $1.0 \leq AF \leq 1.2$.
- TF : Consideration of the temperature dependence of the PDIV – $1.0 \leq TF \leq 1.3$.

In the electrical drive train, which serves as a testing device for the coils, the electric machine and the power electronic inverter are connected using a short cable of 100 mm length. Therefore, the overshoot factor OF is set to its minimum of 1.1. All other factors are set to their maximum to achieve a worst case scenario. This yields a minimum PDIV of $U_{pkpk,min} = 1416$ V for a dc link voltage of $U_{dc} = 300$ V. For initial measurements in this study a commercial stator tester (*Schleich MTC 3*) which can supply a sinusoidal voltage with a frequency of 50 Hz and a unipolar pulse voltage (Fig. 7 a) and b) is employed. The inverter however causes a bipolar pulse (Fig. 7 c)) voltage in the winding. Therefore, for further studies also a bipolar pulse voltage generator which is introduced in [3] is applied.

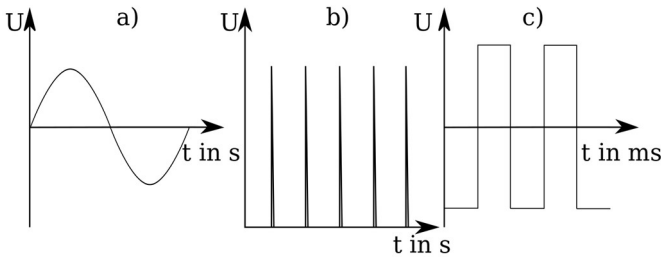


Fig. 7: Sinusoidal voltage (a), unipolar pulse voltage (b) and bipolar pulse voltage (c).

A. PDIV Measurements for Concept A

The *Paschen* curve and its mathematical description, the *Townsend* equation

$$U_{Paschen} = \frac{B \cdot p \cdot d}{\ln(A \cdot p \cdot d) - \ln(\ln(1 + \gamma^{-1}))} \quad (2)$$

can be used to determine the minimum voltage $U_{Paschen}$ which is required for discharge processes. It depends on the air pressure p , the distance between the electrodes d as well as the parameters A and B that depend on the surrounding gas and are well known for air. γ is the second *Townsend* coefficient. It depends on the properties of the electrode surface. In [9] the second *Townsend* coefficient for polyamide-imide is given.

At normal pressure (1013 hPa), the *Paschen* curve's minimum for a combination of air and polyamide-imide occurs at an effective voltage of 436 V or a peak-to-peak voltage of 1234 V.

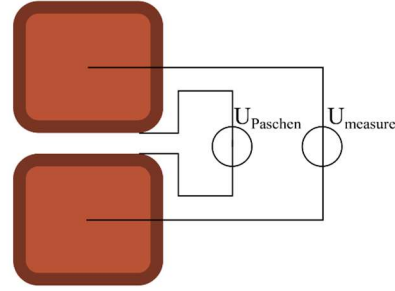


Fig. 8: Comparison of the measured voltage $U_{measure}$ and the calculated voltage $U_{Paschen}$ in a conductor arrangement.

The voltage at the *Paschen* minimum $U_{Paschen,min}$ refers to the potential difference between the insulation surfaces. During PDIV measurements however the voltage between the conductors $U_{measure}$ is measured (Fig. 8). For the simplified arrangement of an ideal capacitor, the relation between $U_{measure}$ and $U_{Paschen,min}$ is given by

$$U_{measure} = U_{Paschen,min} \cdot \left(1 + \frac{2 \cdot d_{Iso}}{\epsilon_{r,Iso} \cdot d_{Air}} \right) \quad (3)$$

where d_{Iso} is the insulation thickness, d_{Air} is the distance between the insulation surfaces and $\epsilon_{r,Iso}$ is the permittivity of the insulation material.

During the production of the specimens, the deformation process causes an increase of the circumference of the conductor cross section and will therefore decrease the insulation thickness. The geometry of the conductor can be approximated by a rectangle, joint to two circle segments (Fig. 9).

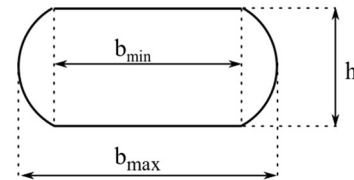


Fig. 9: Schematic drawing of formed conductor.

TABLE II. DIMENSIONS OF FORMED CONDUCTORS

Parameter	Conductors with a desired height of 2 mm	Conductors with a desired height of 4 mm
b_{min}	7.7 mm	3.7 mm
b_{max}	8.2 mm	5.7 mm
h	2.6 mm	4.2 mm

The parameters b_{\min} , b_{\max} and h measured for the conductors with a desired height of 2 mm and 4 mm respectively are displayed in Tab. II.

Assuming, that the insulation thickness changes equally around the circumference, the insulation thickness d_{iso} is estimated for a formed grade 3 enameled round shaped wire with a diameter of 5 mm. For the conductors with a desired height of 2 mm $d_{\text{iso}} = 60.6 \mu\text{m}$ and for the conductors with a desired height of 4 mm $d_{\text{iso}} = 66.3 \mu\text{m}$ is achieved. Applying eq. (2), a PDIV of 2753 V for the 2 mm conductors and a PDIV of 2898 V for the 4 mm conductors are calculated.

The PDIV is measured employing a sinusoidal voltage with a frequency of 50 Hz. Measured and calculated PDIVs for concept A are displayed in Fig. 10. In both cases the PDIV decreases the more the specimens are deformed. However, the calculated PDIV drops less significant than the measured PDIV. The insulation thickness is not evenly distributed around the conductor. In Fig. 12 a close-up of the conductor is displayed. The conductor surface is brighter in the center because, the copper is closer to the enamel surface in this area. Therefore, PD is more likely to occur.

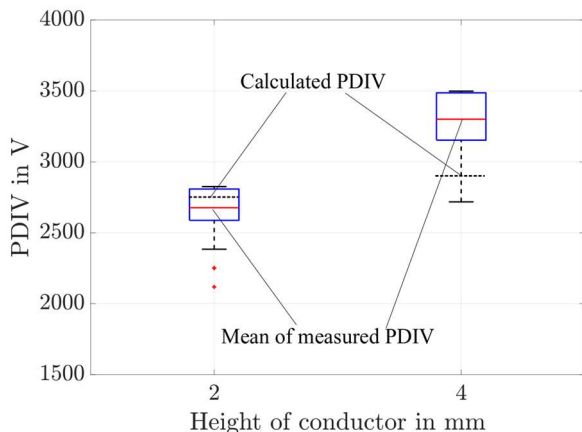


Fig. 10: PDIVs of specimens with different heights of the formed conductor.

In Fig. 11 the PDEV is displayed. The mean PDIV is 19 % higher than the mean PDEV for the specimens with a desired height of 2 mm and 11 % higher for the specimens with 4 mm height. The difference between PDIV and PDEV is therefore smaller than predicted by the standard (25 %) [2].

The large force stressing the enamel during the forming process also influences the mechanical properties of the enamel. In Fig. 13 a close-up of the angle which represents the end winding is displayed.

On the outer part of the curve, a crack in the enamel is displayed. On the inner part a ripple of the insulation can be spotted. Due to these defects, Concept B is focused in the following.

B. PDIV Measurements for Concept B

For concept B specimens that are insulated using *Lankwitzer EvoProtect 130*, a two-component epoxy-based varnish, are tested. The measured PDIVs are given in Fig. 14. As the coils are designed to be employed in inverter driven machines, bipolar pulse voltages are applied and compared to the results that are obtained using sinusoidal voltages from a commercial

stator tester. The parameters of the pulse voltage are listed in Tab. III.

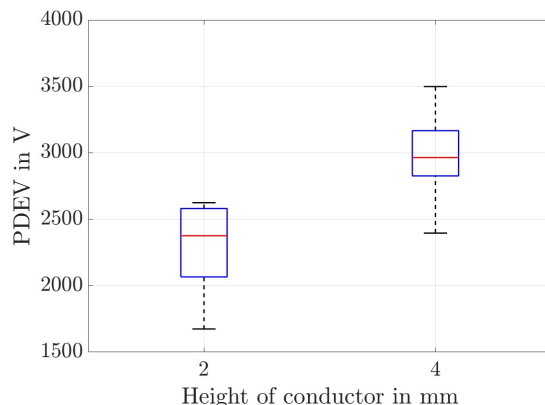


Fig. 11: PDEVs of specimens with different heights of the formed conductor.

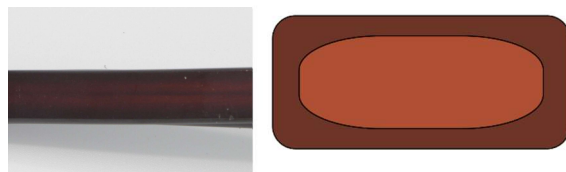


Fig. 12: Close-up of formed conductor: The enamel in the center is notably thinner (left), schematic drawing of the cross section of a formed wire (right).



Fig. 13: Close-up of a defect in the surface insulation.

TABLE III. DIMENSIONS OF FORMED CONDUCTORS

Parameter	Value
Switching frequency f_{sw}	16 kHz
Voltage risetime t_r	80 ns
Voltage slew rate du/dt at $U_{\text{dc}} = 1200 \text{ V}$	29 kV/ μs
Overshootfactor OF	1.066

All specimens meet the requirements that are defined by eq. (1). The PDIVs that are achieved using the bipolar pulse voltage are significantly lower than the PDIVs for the sinusoidal voltage, even though both test voltages are suitable according to [2]. The relation between PDEVs at sinusoidal voltage respectively at pulse voltage is the same (Fig. 15). The coefficient of variation CV is defined by the fraction of standard deviation σ and expected value μ :

$$CV = \frac{\sigma}{\mu} \quad (4)$$

It is used to compare the spread of measured PDIVs of classical round wires and coated specimens from concept B. For a measurement of 20 conventional *Dahréntråd Damid*

200 wires of grade 2, a coefficient of variation of $CV = 0.112$ is achieved and for 20 specimens of the concept B, a coefficient $CV = 0.093$. For conventional round wires twisted pair specimens are applied which are produced under well defined conditions [10]. The taping process that is used to form the specimens which are presented in Fig. 5 is performed manually and is therefore prone to deviations. In Fig. 16 the normalized PDIVs of the conventional wire and the coated specimens are compared. The spread of the measured PDIVs of the concept B insulation is in the same range as for a conventional insulation system. Therefore, it is expected that quality deviations of the coated specimens are not larger than the quality deviations of standard enameled round wires.

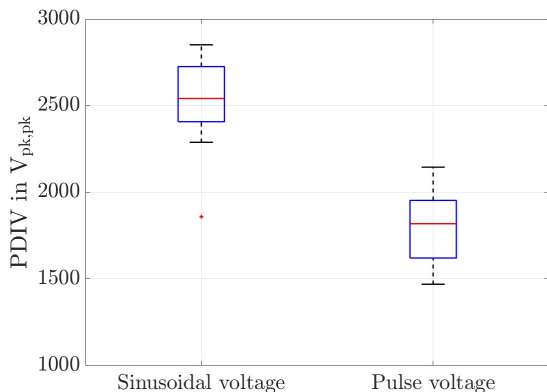


Fig. 14: Comparison between PDIVs of specimens under sinusoidal and under bipolar voltage load.

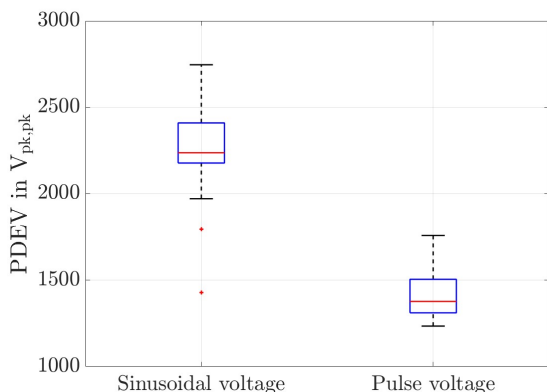


Fig. 15: Comparison between PDEVs of specimens under sinusoidal and under bipolar voltage load.

The insulation thickness of the specimens from concept A is in the range of the insulation thickness of the insulation of the round shaped enameled wire which is used as a raw material. Therefore, it meets the requirements for the defined coil geometry.

For the specimens produced for concept B, particular attention must be paid to the insulation thickness. Measurements of the insulation thickness for coated wire samples show, that the insulation thickness is in the range of the permissible maximum of $80 \mu m$.

While properties such as electrical resistance, mechanical and thermal stress are well tested for conventional insulation materials. These properties are unknown for the epoxy based varnish, which is used for concept B. Therefore, accelerated

lifetime tests considering the entire insulation system are performed.

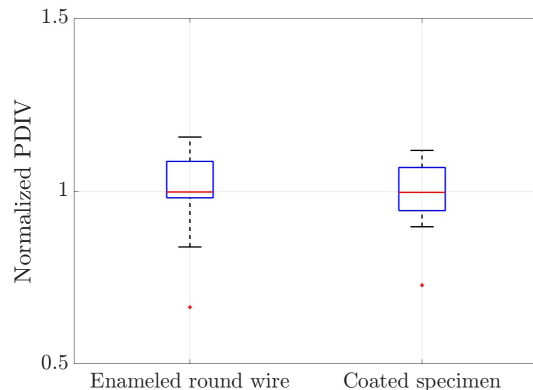


Fig. 16: Normalized PDIV under a sinusoidal voltage load with a frequency of 50 Hz for conventional enameled wires and for coated specimens.

V. ACCELERATED LIFETIME TESTS OF THE INSULATION SYSTEM

Accelerated lifetime tests are performed by increasing the stress on a system beyond the limits of its operating range. Then, the time until a breakdown of the system is measured and mathematical models are applied to determine the expected lifetime in a system that is operated under nominal conditions.

Due to economic reasons, the lifetime tests are not performed using complete stators but so called motorettes. A construction made out of metal sheets is used to simulate the slot of an electrical machine. The developed coil is inserted into the slot along with the remaining insulation system. In this study, first motorettes are built using insulated semi finished coils. Thus, the development of the coil and the insulation system can be parallelized. The resulting motorette is displayed in Fig. 17.

As the insulation system is designed to be PD free, thermal ageing is expected to be the dominant ageing factor. A procedure for cyclic ageing is defined in the standard [10]. The insulation system is alternately exposed to high temperatures, vibrations, which cause high mechanical stress and high humidities. Mechanical stress in electrical machines occurs due to the rotating magnetic field and – in traction drives – due to vibrations from the vehicles body. Due to ambient conditions, traction drives are also likely to be exposed to high humidity.

The combined ageing cycle ensures that all these effects are considered. The test cycle is displayed in Fig. 18.

Before the accelerated ageing is started, an initial diagnostic measurement is performed to detect failures that occur in the production process of the motorette. Subsequently, a pre-conditioning is performed: For 24 hours, the motorettes are subjected to a bipolar pulsevoltage which for the specimens is larger than the minimum acceptable PDIV. A frequency of 16 kHz is chosen, as it equals the maximum inverter frequency. The test is performed to ensure that the insulation system is PD free.

The cyclic tests are performed for three groups of motorettes. The test cycle for these groups differs for the subcycle of thermal ageing. According to the *Dakin* equation, thermal

ageing is accelerated, when high temperatures are applied [11]:

$$L_{\text{Dakin}} = A_{\text{Dakin}} \cdot e^{\frac{B_{\text{Dakin}}}{T}} \quad (5)$$

L_{Dakin} is the predicted lifetime, T is the absolute temperature and A_{Dakin} and B_{Dakin} are material dependent parameters. Subsequently the group of motorettes, which is subjected to the highest temperatures, is aged for the shortest time and vice versa (Tab. IV).

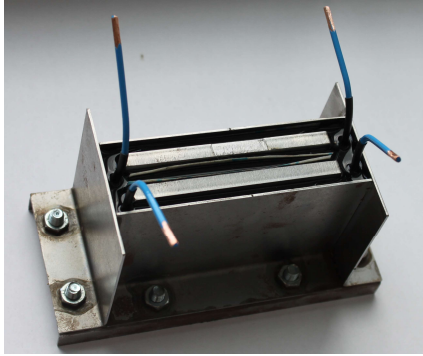


Fig. 17: Motorette with semi finish.

TABLE IV. DIMENSIONS OF FORMED CONDUCTORS

Motorette Group	Temperature in °C	Time in d	Estimated number of cycles
A	150	14	10
B	170	4	10
C	180	2	10

The aim of this procedure is to qualify the insulation system for a thermal class of 120 °C. The temperature for the thermal ageing subcycles is chosen such that the estimated number of cycles until the end of life of the insulation system equals to ten.

In the diagnostic measurement the following parameters are considered:

- Insulation resistance R_{iso} ,
- Capacitance C_{iso} ,
- Loss factor $\tan \delta$ and
- PDIV.

The resistance R_{iso} is measured to detect defects in the insulation leading to a direct short circuit between the two phases or between one phase and the grounded metal arrangement of the motorette, which represents the stator. The capacitance C_{iso} and the loss factor $\tan \delta$ mainly consider the impregnation material. A severe drop of C_{iso} indicates the loss of impregnation material. A change of $\tan \delta$ also occurs in case of the loss of insulation material or if the chemical properties of the impregnation material change. High loss factors must be avoided as they lead to thermal losses of the insulation material when it is subjected to an alternating electric field. They can therefore lead to local hotspots inside the winding.

The PDIV is measured for a sinusoidal and a bipolar pulse voltage. While the other parameters are only considered for a diagnostic purpose, the minimum PDIV serves as an end of life criterion. It is calculated by modifying eq. (1):

$$U_{\text{pkpk,min,ph-ph}} = 2 \cdot U_{\text{dc}} \cdot OF \cdot NF \cdot PD \cdot TF \quad (6)$$

for the phase to phase insulation and

$$U_{\text{pkpk,min,ph-gd}} = 2 \cdot 0.7 \cdot U_{\text{dc}} \cdot OF \cdot NF \cdot PD \cdot TF \quad (7)$$

for the phase to ground insulation.

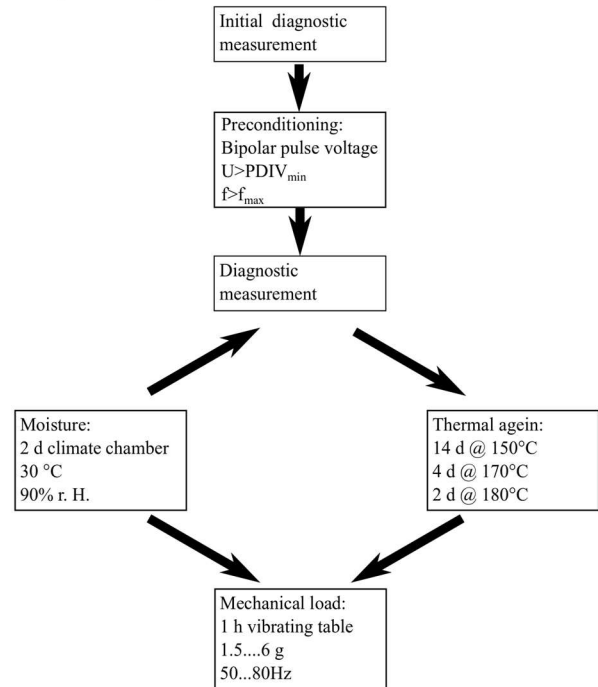


Fig. 18: Test cycle for accelerated thermal ageing of the insulation system.

OF , NF , PD and TF are safety factors to consider overshoot, variation of dc link voltage, the difference of PDIV and PDEV and the operating temperature respectively. The Factor a from eq. (1) is no longer applied. While for conductor arrangements the entire voltage is applied to the interturn insulation, for complete stators and motorettes only a fraction of the test voltage drops between the first turns (Fig. 6). The ageing factor AF is not considered for the ageing tests, as opposing to the conductor setups from section IV PDIVs of already aged specimens are measured. The phase to ground voltage in three phase electrical machines is decreased by a factor of $1/\sqrt{3} \approx 0.577$. However, in inverter driven machines the potential of the star point can vary. This is considered by applying an empirical factor of 0.7 instead of 0.577 in eq. (7). For the minimum PDIVs of the studied insulation system, the following voltages are achieved:

- $U_{\text{pkpk,min,ph-p}} = 1180 \text{ V}$ and
- $U_{\text{pkpk,min,ph-ph}} = 826 \text{ V}$.

As PD causes electrical ageing of the winding and high voltages can cause breakdowns, which lead to an immediate breakdown of the system, the maximum voltage which is applied during PD tests is limited to two times the minimum PDIV.

First results of the lifetime measurement are displayed in Figures 19 to 21. While there is no significant change of the capacitance and the loss factor, the resistance increases slightly after the pre-conditioning and then drops significantly. During the pre-conditioning, the temperature of

the motorette rises due to iron losses. The high temperatures can lead to a curing of the impregnation material. During the first thermal cycle, even higher temperatures are applied to the motorette. The primary insulation therefore starts degrading. Additionally, high humidity is applied prior to the diagnostic measurement, which leads to a decreased resistance. In the second cycle the resistance is only slightly decreased.

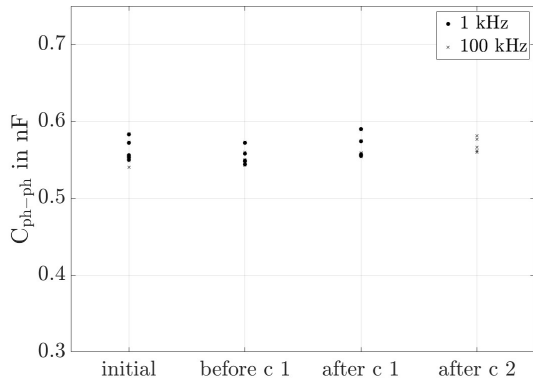


Fig. 19: Capacitance of six motorettes from group A at the initial measurement, before cycle 1 and after cycle 1.

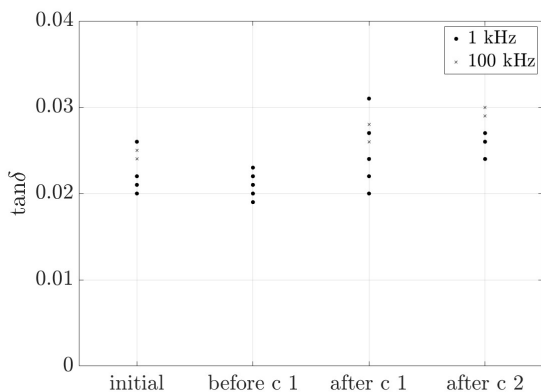


Fig. 20: Loss factor of six motorettes from group A at the initial measurement, before cycle 1 and after cycle 1.

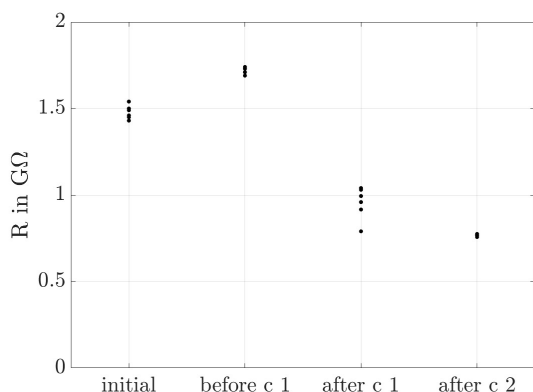


Fig. 21: Insulation resistance of six motorettes from group A at the initial measurement, before cycle 1 and after cycle 1.

All motorettes passed the PDIV tests. No PD is measured for any of the motorettes when the voltage is increased to its limit of two times the minimum PDIV. Therefore, the cyclic ageing tests are continued.

VI. CONCLUSIONS AND FUTURE WORK

It can be noticed, that due to the defects in the insulation, concept A is not a feasible approach for the primary insulation system. Therefore, concept B is further examined. Here, the minimum PDIV of the specimens is 1469 V for a bipolar pulse voltage and 1858 V for the sinusoidal voltage respectively. Therefore, all specimens meet the requirements which are defined based on [2]. However, as there is only little experience with epoxy based coating as primary electrical insulation, further properties to prove the feasibility of the concept such as the temperature index and the ageing behavior must be tested. To ensure the endurance of the concept, currently ageing tests are being performed. First results show, that the insulation can be operated up to 150 °C for short-term operation. To qualify the system for a thermal class of 120 °C for continuous operation, the ageing tests are continued.

REFERENCES

- [1] D. Petrell, A. Braun and G. Hirt: "Comparison of Different Upsetting Processes for the Production of Copper Coils for Wheel Hub Engines", 8th Congress of the German Academic Association for Production Technology (WGP), pp 445-454, Springer, 2018.
- [2] IEC 60034-18-41 ed. I, Rotating electrical machines – Part 18-41: Partial discharge free electrical insulation systems (Type I) used in rotating electrical machines fed from voltage converters – Qualification and quality control tests, 2014.
- [3] K. Hameyer, A. Ruf and F. Pauli: "Influence of fast switching semiconductors on the winding insulation system of electrical machines", International Power Electronics Conference (IPEC), pp. 740-745, Niigata, 2018.
- [4] P. Stenzel, P. Dollinger, J. Richnow and J. Franke: "Innovative needle winding method using curved wire guide in order to significantly increase the copper fill factor", 17th International Conference on Electrical Machines and Systems (ICEMS), pp. 3047-3053, Hangzhou, 2014.
- [5] M. Gröninger, F. Horch, A. Kock, H. Peteit, B. Poick, D. Schmidt and F.-J. Wöstmann: "Casting production of coils for electrical machines", 1st International Electric Drives Production Conference, pp. 159-161, Nuremberg, 2011.
- [6] B. Stone, E. Boulter, I. Culbert and H. Dhirani: Electrical Insulation for Rotating Machines, WILEY INTERSCIENCE, 2004.
- [7] EC 60317-0-1:2013: "Specifications for particular types of winding wires - Part 0-1: General requirements - Enamelled round copper wire", September 2013.
- [8] IEC 60172:2015: "Test procedure for the determination of the temperature index of enamelled and tape wrapped winding wires", June 2015.
- [9] L. Lusuardi, A. Cavallini, P. Mancinelli, G. De La Calle Manuel, J. M. Martínez-Tarifa and G. Robles: "Design criteria for inverter-fed Type 1 motors", IEEE International Conference on Dielectrics (ICD), pp. 605-608, Montpellier, 2016.
- [10] IEC IEC 60034-18-21:2012: "Functional evaluation of insulation systems - Test procedures for wire-wound windings - Thermal evaluation and classification", July 2013.
- [11] T. W. Dakin: "Electrical Insulation Deterioration Treated as a Chemical Rate Phenomenon", Transactions of the American Institute of Electrical Engineers, vol. 67, no. 1, pp. 113-122, Jan. 1948.
- [12] IEC 60034-18-42 ed. I, Rotating electrical machines - Part 18-42: Partial discharge resistant electrical insulation systems (Type II) used in rotating electrical machines fed from voltage converters - Qualification tests, 2017.
- [13] B. Hofmann, B. Bickel, P. Bräuer, M. Leder and J. Franke: "Theoretical benefits of powder-coating based insulation layers regarding copper fill factor in electric drives", 6th International Electric Drives Production Conference (EDPC), Nuremberg, 2016, pp. 172-176.
B. Hofmann, S. Spreng, J. Franke and B. Maryniak: "Innovative and energy-efficient insulation technology for the production of electric drives", 4th International Electric Drives Production Conference (EDPC), Nuremberg, 2014, pp. 1-5.